Supplemental material to *"The relative contributions of store-operated and voltage-gated Ca^{2+} channels to the control of Ca^{2+} oscillations in airway smooth muscle"*

August 2, 2016

Model equations

The differential equations are:

$$\begin{aligned}
\dot{c} &= J_{\mathrm{Release}} - J_{\mathrm{Serca}} - \delta\left(J_{\mathrm{VGCC}} + J_{\mathrm{ROCC}} + J_{\mathrm{SOCC}} + J_{\mathrm{PM}}\right), && (1)\\
\dot{c}_{\mathrm{b}} &= \gamma_1(J_{\mathrm{IPR}} - J_{\mathrm{Diff}}), && (2)\\
\dot{c}_{\mathrm{t}} &= -\delta\left(J_{\mathrm{VGCC}} + J_{\mathrm{ROCC}} + J_{\mathrm{SOCC}} + J_{\mathrm{PM}}\right), && (3)\\
\dot{h}_{42} &= \lambda_{h42}\left(\frac{k_{-42}^3}{c_{\mathrm{b}}^3 + k_{-42}^3} - h_{42}\right), && (4)\\
\dot{P}_{\mathrm{so}} &= \frac{1}{T_{\mathrm{Socc}}}\left(P_{\mathrm{so}}^{\infty} - P_{\mathrm{so}}\right), && (5)\\
\dot{V} &= -\frac{1}{C_{\mathrm{m}}}\left(J_{\mathrm{PM}} + J_{\mathrm{ROCC}} + J_{\mathrm{SOCC}} + J_{\mathrm{VGCC}} + I_{\mathrm{Kdr}} + I_{\mathrm{ClCa}}\right.\\
&\quad \left. + I_{\mathrm{bK}} + I_{\mathrm{bNa}} + I_{\mathrm{NaK}} + I_{\mathrm{KCa}}\right). && (6)
\end{aligned}$$

The variable c is the Ca^{2+} concentration in the cytosol, c_{b} is the Ca^{2+} concentration in a microdomain around the cytosolic side of the IPR to account for high Ca^{2+} after release, details can be found in Cao et al. (2014). The variable c_{t} is the total Ca^{2+} concentration in the cell, h_{42} is a gating variable involved in the opening and closing of the IPR, P_{so} is a gating variable for the store-operated Ca^{2+} channel as introduced in Wang et al. (2010) and V is the voltage across the plasma membrane.

The Ca^{2+} concentration in the SR is determined by the conservation relationship $c_t = c + c_b/\gamma_1 + c_s/\gamma_2$, where γ_1 is the volume ratio between cytoplasm and microdomain around the IPR and γ_2 is the volume ratio between cytoplasm and SR. The Ca^{2+} concentration in the SR is:

$$c_s = \gamma_2 \left(c_t - c - \frac{c_b}{\gamma_1} \right). \tag{7}$$

The release of Ca^{2+} from internal stores into the cytosol is given by

$$\begin{aligned} J_{\text{Release}} &= J_{\text{diff}} + J_{\text{leak}} + J_{\text{RyR}}, \\ J_{\text{diff}} &= k_{\text{diff}}(c_b - c), \\ J_{\text{leak}} &= k_{\text{leak}}(c_s - c), \\ J_{\text{RyR}} &= k_{\text{RyR}} P_{\text{RyR}}(c_s - c), \end{aligned} \tag{8}$$

where J_{diff} is the Ca^{2+} current from the microdomain around the IPR, J_{leak} is a generic leak from the sarcoplasmic reticulum to the cytosol and J_{RyR} is the current through the Ryanodine receptor.

A microdomain around the channel mouth on the cytosolic side of the IPR yields a more realistic Ca^{2+} concentration after Ca^{2+} release through the IPR. The released Ca^{2+} diffuses out of the microdomain into the cytosol. Without the microdomain, the Ca^{2+} concentration at the channel mouth of the IPR is the same as c, yielding less accurate IPR kinetics. Details of the IPR model and the microdomain are in Cao et al. (2014).

The current through the IPR is:

$$J_{\text{IPR}} = k_{\text{IPR}} \frac{D q_{26}}{q_{62} + q_{26}} (c_s - c_b). \tag{9}$$

The pump is modeled by

$$J_{\text{Serca}} = \frac{V_s c^{\text{ns}}}{K_s^{\text{ns}} + c^{\text{ns}}}, \tag{10}$$

which is taken from Chandrasekera et al. (2009).

Three different channels types are taken into account for Ca^{2+} influx. The ROCC and the SOCC are given by:

$$J_{\text{ROCC}} = V_{\text{rocc}} p (V - E_{\text{Ca}}), \tag{11}$$

$$J_{\text{SOCC}} = V_{\text{socc}} P_{\text{so}} (V - E_{\text{Ca}}). \tag{12}$$

In absence of an established detailed model for the ROCC, it is modeled by a linear function of $InsP_3$ (p) as has previously been done (Wang et al., 2010), (Croisier et al., 2013), augmented by a voltage-dependent forcing term. The model for SOCC has been adapted from Croisier et al. (2013) with a voltage-dependent forcing term added. The SOCC respond via the open probability on a time scale, given by T_{socc}, to changes in the Ca^{2+} concentration in the SR.

The model for the VGCC has been previously suggested by Wang et al. (2010) and is written as

$$J_{\mathrm{VGCC}} = g_{\mathrm{Ca}} m_{\mathrm{Vocc}}^2 V_{\mathrm{Ca}}, \tag{13}$$

where m_{Vocc} is a gating variable and V_{Ca} represents the driving force, derived from a Goldman-Hodgkin-Katz equation (Eq. (23)).

The plasma membrane pump for the extrusion of Ca^{2+} is modeled by

$$J_{\mathrm{PM}} = \frac{V_{\mathrm{p}} c^{\mathrm{np}} - \omega [\mathrm{Ca}]_{\mathrm{ext}}}{K_{\mathrm{p}}^{\mathrm{np}} + c^{\mathrm{np}}}, \tag{14}$$

which contains a term that depends on the extracellular Ca^{2+} concentration $[\mathrm{Ca}]_{\mathrm{ext}}$.

The fluxes across the plasma membrane are measured in nA, where the fluxes that contribute to the Ca^{2+} concentrations are effective fluxes measured in $\frac{\mu \mathrm{M}}{s}$. The factor δ takes the different units into account and has been estimated by

$$\delta = \frac{1}{2\mathrm{F} \cdot \mathrm{Vol}} \cdot 10^{-3} \approx 1.449 \frac{\mathrm{mol}}{\mathrm{C\ l}}, \tag{15}$$

where F is the Faraday constant and Vol is the volume of the cell in mol. The volume has been approximated to be $\mathrm{Vol} = 3.58 \cdot 10^{-12} l$ based on the data in (Jones et al., 2014). Since most of the Ca^{2+} influx is directly taken up by buffers and only the free cytosolic Ca^{2+} is taken into account in Eq. (1) and Eq. (3), it is estimated that the effective flux is 1000 times smaller than the flux across the cell membrane. A model for effective fluxes take fast, linear buffers into account. More complicated buffer kinetics would have to be explicitly included and is beyond the scope of this article.

The following ion channels in the plasma membrane are taken as modeled

in Roux et al. (2006). The background currents for K^+ and Na^+ are

$$I_{\mathrm{bK}} = g_{\mathrm{bK}}(V - E_{\mathrm{K}}), \tag{16}$$

$$I_{\mathrm{bNa}} = g_{\mathrm{bNa}}(V - E_{\mathrm{Na}}). \tag{17}$$

The delayed rectifier K current is

$$I_{\mathrm{Kdr}} = g_{\mathrm{Kdr}}(\gamma_{\mathrm{KSS}} + (x_{i1,\infty} + x_{i2,\infty})(1 - \gamma_{\mathrm{KSS}}))x_{\mathrm{a},\infty}^2(V - E_{\mathrm{K}}), \tag{18}$$

with activation gating variable x_a and inactivation gating variables x_{i1} and x_{i2} (Roux et al., 2006). The Ca^{2+}-activated K^+ current is

$$I_{\mathrm{KCa}} = g_{\mathrm{KCa}}x_{\mathrm{Ca1},\infty}B(V - E_{\mathrm{K}}), \tag{19}$$

with gating variables $x_{\mathrm{Ca1},\infty}$ and B, which is taken from Roux et al. (2006). The Na^+ K^+ exchanger is

$$I_{\mathrm{NaK}} = I_{\mathrm{NaK,max}}\frac{K_{\mathrm{ext}}}{K_{\mathrm{mK}} + K_{\mathrm{ext}}}\frac{\mathrm{Na}_{\mathrm{int}}}{K_{\mathrm{mNa}} + \mathrm{Na}_{\mathrm{int}}}. \tag{20}$$

The Ca^{2+}-activated Cl^- channel is given by

$$I_{\mathrm{ClCa}} = g_{\mathrm{Cl}}\frac{V - E_{\mathrm{Cl}}}{1 + (\mathrm{Ca}_{\mathrm{CT}}/c)^3}. \tag{21}$$

Functions and parameters can be found below.

In order to simplify the model, we have eliminated variables x_{i1}, x_{i2}, x_a and B by quasi-steady-state reduction, as outlined in Boie et al. (2016), and replaced them by the functions shown below. This simplification does not affect the qualitative dynamics.

The model by Roux et al. (2006) take non-specific Ca^{2+}, K^+ and Na^+ channels into account but mention that their contributions are very small. We confirmed that non-specific ion channels as well as an additional background Ca^{2+} channel contribute very little to membrane fluxes. Hence, we have decided to omit these channels.

Functions and parameters

The open state of the ryanodine receptor is determined by

$$P_{\mathrm{RyR}} = \left(k_{\mathrm{ryr0}} + \frac{k_{\mathrm{ryr1}} c^3}{k_{\mathrm{ryr2}}^3 + c^3} \right) \frac{c_{\mathrm{s}}^4}{k_{\mathrm{ryr3}}^4 + c_{\mathrm{s}}^4}, \tag{22}$$

which is taken from Wang et al. (2010).

$\mathbf{InsP_3}$ receptor

Functions determining the IPR kinetics are

$$\begin{aligned}
a_{42} &= 1.8 \frac{p^2}{p^2 + 0.34}, \\
a_{24} &= 1 + \frac{5}{p^2 + 0.25}, \\
V_{24} &= 62 + \frac{880}{p^2 + 4}, \\
V_{42} &= \frac{110 p^2}{p^2 + 0.01}, \\
k_{42} &= 0.49 + \frac{0.543 p^3}{p^3 + 64}, \\
k_{-42} &= 0.41 + 25 \frac{p^3}{p^3 + 274.6}, \\
c_{\mathrm{p}} &= c_{\mathrm{p0}} c_{\mathrm{s}} / 100, \\
h_{24,\infty} &= \frac{k_{-24}^2}{c_{\mathrm{p}}^2 + k_{-24}^2}, \\
m_{42,\infty} &= \frac{c_{\mathrm{b}}^3}{c_{\mathrm{b}}^3 + k_{42}^3}, \\
m_{24,\infty} &= \frac{c_{\mathrm{p}}^3}{c_{\mathrm{p}}^3 + k_{24}^3}, \\
q_{42} &= a_{42} + V_{42} m_{42,\infty} h_{42}, \\
q_{24} &= a_{24} + V_{24} (1 - m_{24,\infty} h_{24,\infty}), \\
\lambda_{h_{42}} &= (1 - D) L + D H, \\
D &= \frac{q_{42}(q_{62} + q_{26})}{q_{42} q_{62} + q_{42} q_{26} + q_{24} q_{62}}.
\end{aligned}$$

The detailed derivation and explanation of these functions can be found in Cao et al. (2014).

Membrane fluxes

The Nernst potentials of the ions Ca^{2+}, Na^+, K^+ and Cl^- are

$$E_{\mathrm{Ion}} = \frac{RT}{nF} \log\left(\frac{[\mathrm{Ion}]_{\mathrm{ext}}}{[\mathrm{Ion}]_{\mathrm{int}}}\right),$$

where n is two for Ca^{2+}, one for Na^+ and K^+ and minus one for Cl^-.

The steady-state open probability of the store-operated Ca^{2+} channel is

$$P_{\mathrm{so}}^{\infty} = \frac{K_{\mathrm{Socc}}^4}{K_{\mathrm{Socc}}^4 + c_{\mathrm{s}}^4}.$$

The functions for the VGCC are (Wang et al., 2010):

$$\begin{aligned} m_{\mathrm{Vocc}} &= \frac{1}{1+\exp(-(V-V_{\mathrm{m}})/k_{\mathrm{m}})}, \\ V_{\mathrm{Ca}} &= V\frac{c - \mathrm{Ca}_{\mathrm{ext}}\exp(-2VF/(RT))}{1-\exp(-2VF/(RT))}. \end{aligned}$$

The functions for the delayed rectifier K^+ current are (Roux et al., 2006):

$$\begin{aligned} x_{i1,\infty} &= \frac{1}{1+\exp((V+4.3)/7.5)}, \\ x_{i2,\infty} &= \frac{1}{1+\exp((V+4.3)/7.5)}, \\ x_{\mathrm{a},\infty} &= \frac{1}{1+\exp((5.5-V)/6)}. \end{aligned}$$

The functions for the Ca^{2+}-activated K^+ current are (Roux et al., 2006):

$$\begin{aligned} K_1 &= 0.85\exp(0.04V), \\ K_{-1} &= 0.24\exp(-0.012V), \\ K_2 &= 0.000275\exp\left(\frac{-1.51VF}{RT}\right), \\ K_4 &= 0.0000125\exp\left(\frac{-1.99VF}{RT}\right), \\ x_{\mathrm{Ca1},\infty} &= \frac{c^2 + K_4 c}{c^2 + K_4 c(1+(\alpha/\beta)) + K_4 K_2(\alpha/\beta)}, \\ B &= \frac{K_1 c x_{\mathrm{Ca1},\infty}}{K_{-1}}. \end{aligned}$$

Parameter values can be found in Table 1.

Additional model validation simulations

In this section we show simulations demonstrating the consistency with previous experimental observations and models by (Wang et al., 2010; Croisier et al., 2013). In particular,

- oscillations induced by agonists do not change significantly if the ASMC is depolarized by KCl (cf. Fig. S1A and Fig. 4C of Wang et al. (2010)). Furthermore, the frequency of depolarization-induced oscillations increases significantly in the presence of $InsP_3$ (cf. Fig. S1B and Fig. 4F of Wang et al. (2010)).
- Stimulation by agonist followed by treatment of the PCLS by ryanodine and caffeine increases the Ca^{2+} sensitivity of RyR and locks them in an open state, emptying the SR (cf. Fig. S2 and Fig. 3B in Croisier et al. (2013)).
- Treatment with CPA impairs SERCA pumps, which results in an increased plateau of Ca^{2+} and the stop of oscillations (cf. Fig. S3 and Fig. 6A in Croisier et al. (2013)).

Sensitivity of parameters for relative conductivity of SOCC and VGCC

In this section we study the sensitivity of model validation simulations on the relative conductances of SOCC and VGCC. To this end, we keep the total current through SOCC and VGCC at rest fixed. The current through SOCC is $J_{\mathrm{SOCC},0} = 0.0177$ nA, the current through VGCC is $J_{\mathrm{VGCC},0} = 0.0229$ nA and the total current through both types of channels is $J_0 = 0.0406$ nA. Introducing the parameter Δ allows to shift the relative contributions by varying Δ such that the resting current through both channel types combined stays constant. The modified expression for the Ca^{2+} influxes is

$$J = \Delta \cdot J_{\mathrm{VGCC}} + J_{\mathrm{ROCC}} + \frac{J_0 - \Delta \cdot J_{\mathrm{VGCC},0}}{J_{\mathrm{SOCC},0}} J_{\mathrm{SOCC}} + J_{\mathrm{PM}}, \tag{23}$$

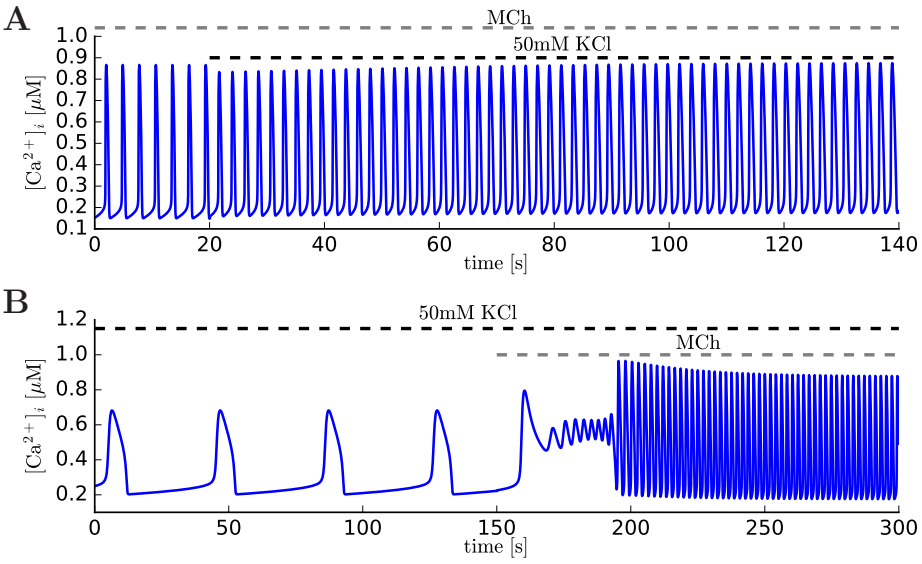

Figure S1: **A:** Stimulation by agonist $[InsP_3] = 0.05\mu M$ followed by depolarization is in good agreement with experimental observations (cf. Fig 4C of Wang et al. (2010)). **B:** Depolarization-induced oscillations speed up significantly in the presence of $[InsP_3] = 0.05\mu M$, cf. Fig 4F of Wang et al. (2010).

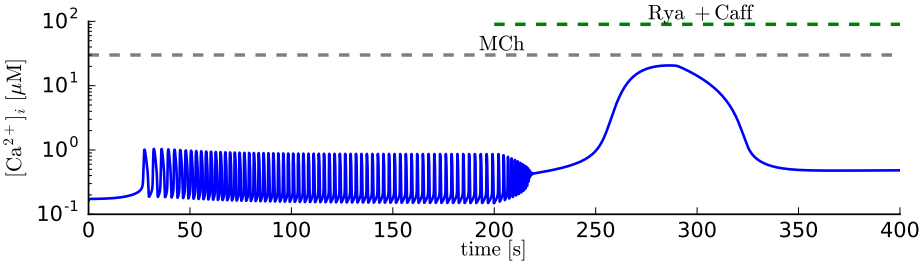

Figure S2: Stimulation by agonist $[InsP_3] = 0.05\mu M$ followed by treatment by ryanodine and caffeine sensitizes RyR to Ca^{2+} and impairs the closing mechanism. The consequence is that the SR loses most its Ca^{2+} and the Ca^{2+} concentration in the cytosol remains elevated (cf. to Fig 3B of Croisier et al. (2013)).

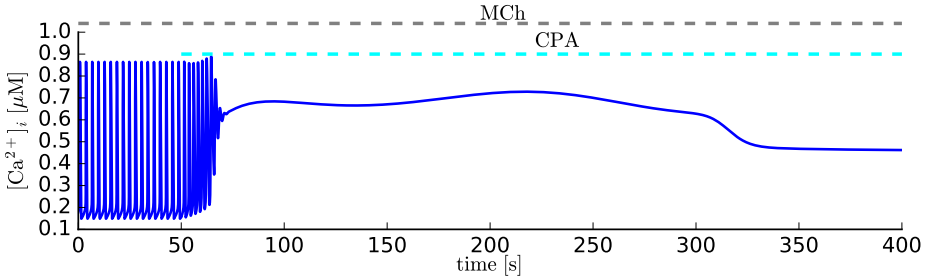

Figure S3: Stimulation by agonist $[InsP_3] = 0.05\mu M$ and treatment with CPA impairs the activity of SERCA pumps abolishing Ca^{2+} oscillations and yielding a plateau of Ca^{2+} (cf. Fig 6A in Croisier et al. (2013)).

which is substituted into Equations (1), (3) and (6). A value of $\Delta = 1.1$ corresponds to an increase in the VGCC current by 10% and a decrease of SOCC current to 87% of its original value. A model parametrized with a 10% higher conductivity of VGCC fails to reproduce the depolarization followed by agonist stimulation (cf. Fig. S1B and Fig. S4A). All other parameter values are unchanged.

Next we test whether a reduced conductivity of VGCC by 10% (corresponding to an increased conductivity of SOCC by 13%) is able to reproduce the model validation simulations. It turns out that a decrease of VGCC by 10% also fails to reproduce the depolarization followed by agonist stimulation (cf. Fig. S1B and cf. Fig. S4B). Furthermore, the shifted balance to a stronger contribution of SOCC leads to different predictions when blocking SOCC during depolarization-induced oscillations (cf. Fig. S4C and Fig. 4B of the article). Deviations of 10% in the relative conductivities of VGCC (correspondingly deviations of 13% in SOCC conductivity) fails to reproduce crucial model validation experiments and hence is deemed unacceptable, leading to a tight bound of the relative contributions of VGCC and SOCC.

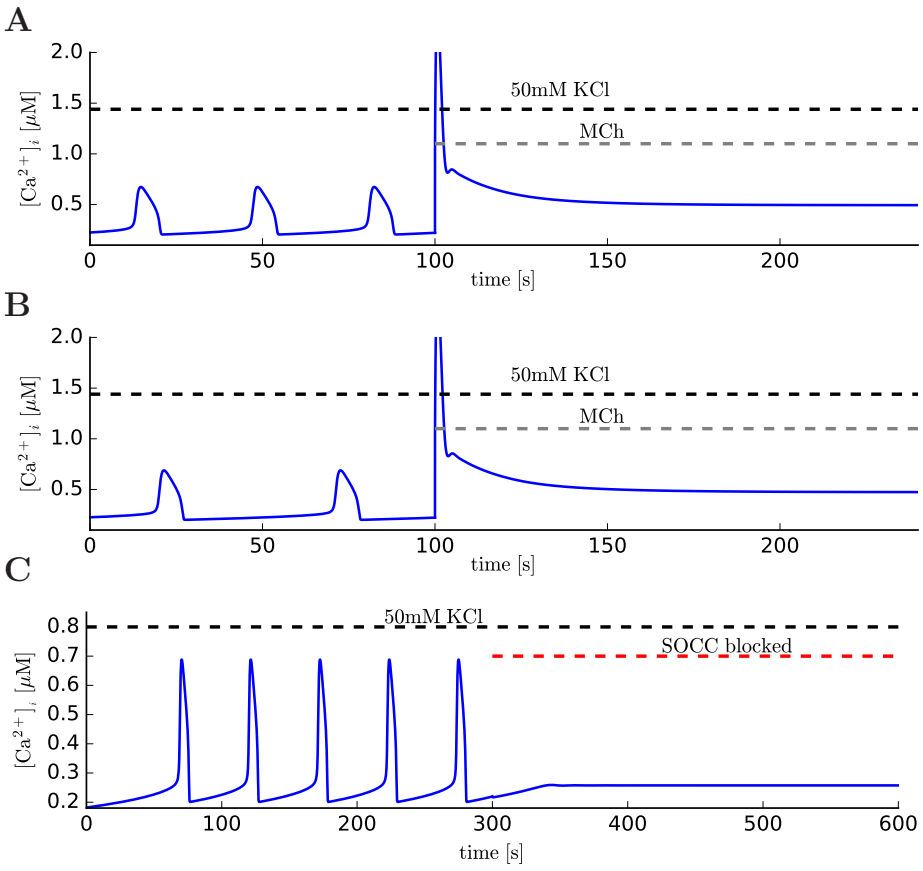

Figure S4: **A:** Stimulation by 50 mM KCl followed by elevated $InsP_3$ ($[InsP_3] = 0.05\mu M$) for $\Delta = 1.1$ fails to reproduce the model validation simulation Fig. S1B corresponding to experimental observations in Fig. 4F of Wang et al. (2010). **B:** The same stimulation protocol fails when the conductivities are changed to a stronger contribution of SOCC ($\Delta = 0.9$). **C:** In addition, when $\Delta = 0.9$ the model predicts that blocking SOCC during depolarization-induced oscillations stops oscillations, which conflicts with the experimental result.

Adjustable parameters			
ω	0.028 $(\mu\text{M})^{-1}$	V_{rocc}	0.0005 μS μmol^{-1}
V_{socc}	0.0015 μS s^{-1}	V_{m}	-18 mV
k_{RyR}	0.11 s^{-1}	δ	1.449 mol $(\text{C l})^{-1}$
g_{Ca}	0.009 μS μM^{-1}	k_{ryr3}	700 μM
k_{ryr1}	0.12 s^{-1}	K_{socc}	450 μM
V_{p}	0.614 nA	k_{m}	17.5 mV
Parameters from Cao et al. (2014)			
c_{p0}	120 μM	γ_1	100
q_{26}	10500 s^{-1}	q_{62}	4010 s^{-1}
γ_2	10	H	20 s^{-1}
L	0.5 s^{-1}	k_{diff}	10 s^{-1}
k_{leak}	0.0032 s^{-1}	K_{s}	0.26 μM
n_{s}	1.75	K_{p}	0.5 μM
k_{42}	0.35 μM	k_{-42}	80 μM
n_{p}	2	k_{IPR}	0.07 (0.05) s^{-1}
V_{s}	13.25 (10) $\mu\text{M}s^{-1}$		
Parameters from Roux et al. (2006) and Roux et al. (2001)			
$[\text{Na}]_{\text{int}}$	12 mM	$[\text{Na}]_{\text{ext}}$	130 mM
$[\text{Cl}]_{\text{ext}}$	140 mM	$[\text{Cl}]_{\text{int}}$	55 mM
g_{Kdr}	0.035 μS	γ_{Kss}	0.15
$[\text{Ca}]_{\text{ext}}$	2 mM	C_{m}	0.00002 μ F
g_{KCa}	2.45 μS	α	280 s^{-1}
β	480 s^{-1}	g_{Cl}	0.01 μS
Ca_{CT}	0.5 μM	K_{mnsCa}	1.2 mM
g_{bK}	0.008729 μS	I_{NaKMax}	0.7 nA
K_{mK}	1 mM	K_{mNa}	40 mM
g_{bNa}	0.003263 μS	R	8314.4621 mJ $(\text{mol K})^{-1}$
F	96485.3415 C mol^{-1}	T	310 K
$[K]_{\text{int}}$	120 (150) mM	$[K]_{\text{ext}}$	8 (5) mM
Parameters from Wang et al. (2010) or Croisier et al. (2013)			
k_{ryr0}	0.0072 s^{-1}	k_{ryr2}	0.33 (0.5) μM
T_{socc}	30 s^{-1}		

Table 1: Parameter values for the model (see discussion in the text for an explanation of the different parameter groupings). Parameters that have been minimally modified from the reference have the reference value shown in parentheses.

References

Boie S, Kirk V, Sneyd J & Wechselberger M (2016). Effects of quasi-steady-state reduction on biophysical models with oscillations. *J. Theor. Biol.* **393**, 16–31.

Cao P, Tan X, Donovan G, Sanderson MJ & Sneyd J (2014). A deterministic model predicts the properties of stochastic calcium oscillations in airway smooth muscle cells. *PLoS Comput. Biol.* **10**, e1003783.

Chandrasekera PC, Kargacin ME, Deans JP & Lytton J (2009). Determination of apparent calcium affinity for endogenously expressed human sarco(endo)plasmic reticulum calcium-ATPase isoform SERCA3. *Am. J. Physiol., Cell Physiol.* **296**, 1105–1114.

Croisier H, Tan X, Perez-Zoghbi JF, Sanderson MJ, Sneyd J & Brook BS (2013). Activation of store-operated calcium entry in airway smooth muscle cells: Insight from a mathematical model. *PLoS ONE* **8**, e69598.

Jones RL, Elliot JG & James AL (2014). Estimating airway smooth muscle cell volume and number in airway sections. Sources of variability. *Am. J. Respir. Cell Mol. Biol.* **50**, 246–252.

Roux E, Noble PJ, Hyvelin JM & Noble D (2001). Modelling of Ca^{2+}-activated chloride current in tracheal smooth muscle cells. *Acta Biotheor.* **49**, 291–300.

Roux E, Noble PJ, Noble D & Marhl M (2006). Modelling of calcium handling in airway myocytes. *Prog. Biophys. Mol. Biol.* **90**, 64–87.

Wang IY, Bai Y, Sanderson MJ & Sneyd J (2010). A mathematical analysis of agonist- and KCl-induced Ca^{2+} oscillations in mouse airway smooth muscle cells. *Biophys. J.* **98**, 1170–1181.